AFRL-SR-AR-TR-04-

0044

REPORT DOCUMENTATION PAGE

1. REPORT DATE *(DD-MM-YYYY)*	2. REPORT TYPE	3. DATES COVERED *(From - To)*
12/08/2004	DURIP Final Performance Report	06/15/02 - 02/14/04

4. TITLE AND SUBTITLE
Optics with Cold Atoms

5a. CONTRACT NUMBER

5b. GRANT NUMBER
F49620-02-1-0207

5c. PROGRAM ELEMENT NUMBER

6. AUTHOR(S)
Lene Hau

5d. PROJECT NUMBER

5e. TASK NUMBER

5f. WORK UNIT NUMBER

7. PERFORMING ORGANIZATION NAME(S) AND ADDRESS(ES)
President and Fellows of Harvard College
Office of Sponsored Research
Holyoke Center, 7th Floor, 1350 Massachusetts Avenue
Cambridge, MA 02138

8. PERFORMING ORGANIZATION REPORT NUMBER
N/A

9. SPONSORING/MONITORING AGENCY NAME(S) AND ADDRESS(ES)
Office of Naval Research
Boston Regional Office
495 Summer Street, Room 627
Boston, MA 02110-2109

10. SPONSOR/MONITOR'S ACRONYM(S)
AFOSR

11. SPONSOR/MONITOR'S REPORT NUMBER(S)
N/A

12. DISTRIBUTION/AVAILABILITY STATEMENT
Unlimited/Unclassified Research/ Financial Assistance

13. SUPPLEMENTARY NOTES
N/A

14. ABSTRACT
For production of novel non-linear excitations in Bose-Einstein condensates, we have enhanced the efficiency and stability of our Bose-Einstein-condensate setup by upgrading one of our primary laser pumps with a modern Verdi V-10 laser system.
Furthermore, we are developing the world's most sensitive single-cold-atom detector based on free-standing carbon nanotubes to ionize neutral atoms. We have generated the facilities necessary for nanotube growth and detailed characterization with the purchase of a Raman microscope. And to test the novel atom sensor, we have built a moving-molasses magneto-optical trap in a geometry tailor-suited to the nanotube detector geometry, involving construction of a highly stable laser source and electro-magnets, with associated power supplies and control circuitry.
In addition, we have applied the DURIP support to produce a continuous source of cold atoms with the highest flux ever obtained (by 1-2 orders of magnitude). This has involved significant upgrades to the optics-table set-up, control electronics and data acquisition system, acquisition of a Fabry-Perot spectrum analyzer, purchase of acousto-optic deflectors with corresponding RF frequency drivers, and custom-building of electronic frequency-locking systems. Characterization of the generated, intense atom beam required similar infrastructure investments, including an acquisition and control computer and electronics with precise timing.

15. SUBJECT TERMS
N/A

16. SECURITY CLASSIFICATION OF:			17. LIMITATION OF ABSTRACT	18. NUMBER OF PAGES	19a. NAME OF RESPONSIBLE PERSON
a. REPORT	b. ABSTRACT	c. THIS PAGE			Lene Hau
					19b. TELEPHONE NUMBER *(Include area code)* 617-496-5967

DURIP Final Report 2004: Optics with Cold Atoms

In the past year we have made significant progress on all of our Air Force sponsored experiments. We have extended our slow light techniques to generate and observe a new class of nonlinear superfluid excitations in Sodium Bose-Einstein condensates. Using a novel combination of magnetic and laser slowing and guiding, we have created the world's most intense cold atom beam which we hope to extend to the quantum degenerate regime for atom optics applications and foundational science. Lastly, we have completed theoretical work exploring the use of carbon nanotubes for low-power single-atom detectors, cold-atom traps and guides and have begun experimental work to test the abilities of these compact, ultra-fast, efficient, and potentially-revolutionary building-blocks for portable devices that exploit atomic phenomena.

INSTRUMENTATION AND FACILITIES DEVELOPED WITH DURIP FUNDING

For production of novel non-linear excitations in Bose-Einstein condensates, we have enhanced the efficiency and stability of our Bose-Einstein-condensate setup by upgrading one of our primary laser pumps with a modern Verdi V-10 laser system.

On another front, we are developing the world's most sensitive single cold-atom detector by taking advantage of the high fields that can be generated at the surface of a single-walled, free standing carbon nanotube to ionize neutral atoms. To this end, we have generated the facilities necessary for nanotube growth and detailed characterization. With the purchase of a Raman microscope system we are able to characterize the chirality, diameter, length, and overall quality of ultra-long carbon nanotubes.

To test the novel atom sensor, we require an atomic beam with high flux density and low temperature, and have developed a moving-molasses magneto-optical trap in a geometry tailor-suited to the nanotube detector geometry. This has involved, for example, the construction of a spectrally pure, highly stable laser source and electro-magnets, with associated power supplies and control circuitry.

In addition, we have applied the DURIP support for the significant enhancement of an existing facility to produce a continuous source of cold atoms with the highest flux ever obtained (by more than an order of magnitude). This has involved upgrades to the optics-table set-up, control electronics, and data acquisition system. Our set-up relies on the spectral purity of our laser sources, which prompted the acquisition of a Fabry-Perot spectrum analyzer, and also on the ability to shift the laser frequency to match a variety of atomic spectral resonances. This has involved the purchase of eight acousto-optic deflectors with corresponding RF frequency drivers. Final locking of our laser system to these spectral resonances required several custom built electronic locking systems. Measurements of the characteristics of the generated, intense atom beam required similar infrastructure investments, including an acquisition and control computer and electronics with precise timing.

ULTRA-SLOW LIGHT AND BOSE-EINSTEIN CONDENSATION ACHIEVEMENTS

In the summer of 2003 we had just completed a complex set-up facilitating studies of vortex dynamics in sodium Bose-Einstein condensates (BECs) at our new laboratory at Harvard University. Our apparatus had been specifically developed to engineer collisions between nonlinear excitations in these cold gas quantum fluids. Since then, we have observed grey soliton collisions, quantized vortex ring collisions, soliton – vortex ring collisions, and the evolution of novel hybrid structures comprising solitons and vortex rings. These findings are detailed in [Ref. 1].

In order to create the solitons and vortices, we draw on our previously developed slow light techniques ([Ref. 2]). A 'coupling' laser beam illuminates the entire BEC, save the central portion. We then inject two counter-propagating light pulses into a BEC, as depicted in Fig. 1 (a). The pulses slow down, spatially compress, and collide from two sides with the *double-light roadblock*, an extension of the *light roadblock* developed for [Ref. 3]. Upon arriving at the roadblock, the pulses compress even further, both creating extremely narrow depletions in the density of trapped atoms, also seen in Fig. 1 (c). Density dips emanating from these defects turn into quantum shock waves. Solitons, non-dispersive collective excitations in the form of narrow density depletions, shed from the latter. If the BEC remains trapped, the solitons are forced to decay into a collection of vortex rings and sound waves via the 'snake' instability. However by switching off the confining trap, the atom cloud expands so that we slowly adjust the degree of nonlinearity in the medium. In this way, rather than complete a full decay, some solitons collide with already-created vortex rings resulting in complex hybrid structures with vortex rings embedded in them.

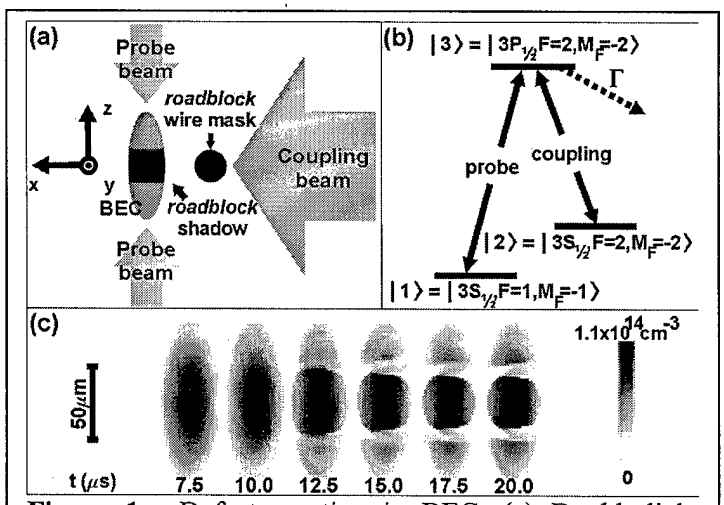

Figure 1. Defect creating in BEC. (a) Double-light roadblock set-up. (b) Slow light energy level diagram. (c) Simulated density plots of defect creation.

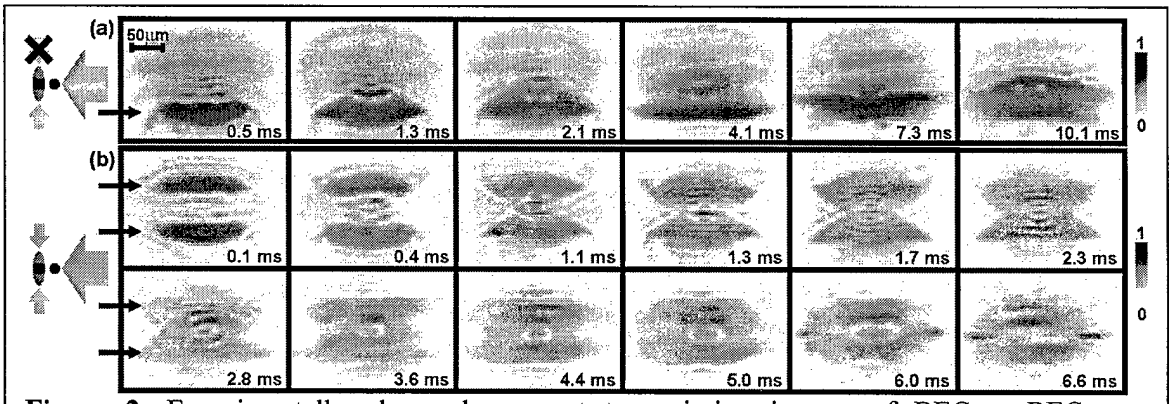

Figure 2. Experimentally observed resonant transmission images of BECs. BECs are illuminated with coupling and probe pulse(s). In (a), one probe pulse is hitting the cloud and in (b) there are two, schematically indicated on the left side of the figure. Times refer to duration of in-trap evolution. Though the cloud is subsequently allowed to expand for 19.9 ms. Arrows indicate initial defect planes.

We have induced collisions of these topological excitations in our experimental apparatus, giving rise to the rich and non-trivial compound structures seen Fig. 2. Vortex rings within the white segments of low density act as 'phantom' propellers in these structures, assisting in their locomotion and changing their shape. When vortex rings within separate segments get too close to one another, we are able to watch them

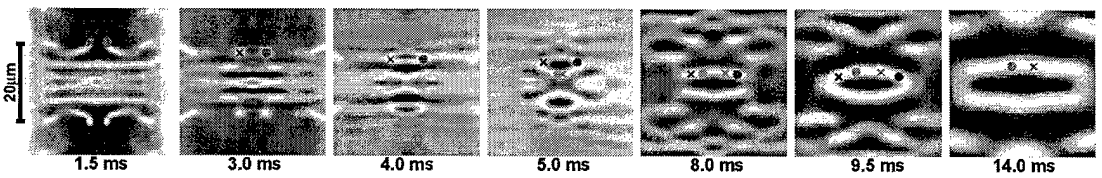

Figure 3. Simulation of soliton vortex-ring dynamics during expansion after a 3.0 ms in-trap evolution. Expansion duration is listed below each frame. Only solitons propagating downward from the top defect are shaded in order to help track their movement from frame to frame. Pairs of dots and crosses of the same color indicate cores of a given vortex ring and are shown for the top half of the frames only.

annihilate, again changing the shape of the hybrid structures. We are the first experimentalists to observe such compound excitations in BECs and to explore the connections between solitons and vortices in this way. These experiments require the utmost precision and control and are on the cutting edge of quantum fluid manipulation and exploration.

The theoretical simulations that we have done allow us to explore the expansion dynamics of the BECs following trap switch-off (when the features are so small that they cannot be directly imaged experimentally). In Fig. 3, we show the simulated evolution of a condensate as it expands (following a 3.0 ms in-trap duration). This sequence aids in elucidating the nature of the experimentally observed structures, particularly via the phase information. As examples, we note the soliton soliton collision at 1.5 and 3.0 ms of expansion, the soliton vortex-ring collision at 5.0 ms, and the vortex-ring vortex-ring collision that leads to annihilation in between the final two frames. These vortex rings

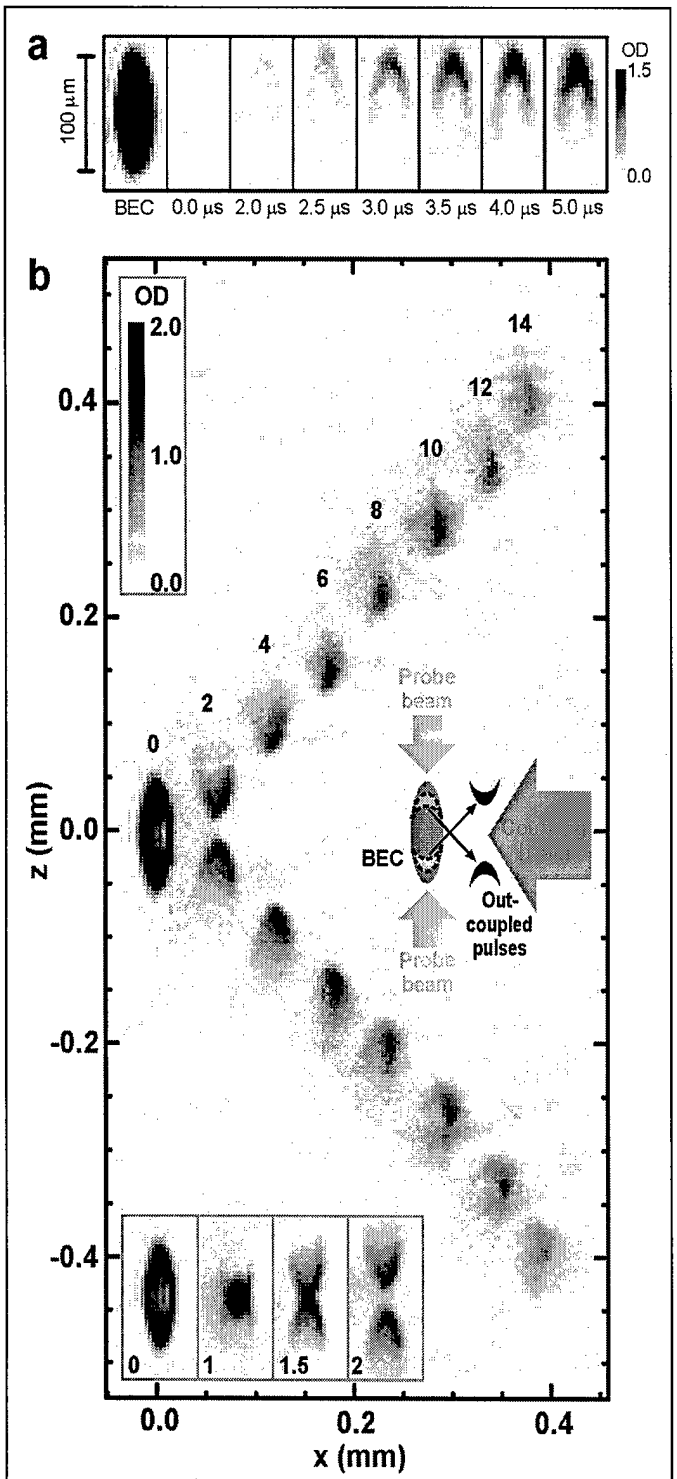

Figure 4. Pulsed atom laser. Absorption images or the out-coupled atoms from our BEC using stopped light in the fashion shown in the inset schematic. In (a), we show the progress of the slow light pulse traveling through the BEC. In (b), we show the outcoupled coherent atom pulses traveling in space.

form parts of the aforementioned hybrid structures and mediate the break-up of the low-density shell comprising soliton and vortex-ring components, seen in Figs. 2 and 3. These sorts of structures are still confounding to many experts in quantum fluid dynamics. The detail in these micron-sized formations and the robustness with which they can be created are a result of the care with which the experiment is effectuated.

Using the same geometry of laser beams as in our superfluid experiments mentioned above, we are able to perform stopped light experiments. As opposed to the results in [Ref. 4] in which we minimized atom recoil by having the probe and coupling beams co-propagate, we are here able to out-couple coherent matter waves from our primary condensate with high directional sensitivity. The emitted matter wave trajectory is a result of the momentum recoils of its constituent atoms from the probe and coupling beams and therefore heads off at a 45 degree angle, as seen in Fig. 4. These experimental findings are detailed in a review of our work, [Ref. 5], and may prove to be of importance in atom interferometry experiments to come. It might also suggest a way to create a directional coupler for light pulses rather than matter waves if one were to transfer the momentum kick from the atoms back to a light field.

RUBIDIUM COLD ATOMIC BEAM EXPERIMENT

In addition to our current

set-up, which is designed to generate BECs for superfluid and atom interferometric experiments, we are in parallel pursuing and experiment for the production of a continuous beam of condensed atoms. Towards this ambitious goal, in our cold atomic beam set-up [Ref. 6], we have been able to produce a continuous beam of rubidium atoms with an unprecedented total flux of 3.2×10^{12} (1.7×10^{12}) atoms/sec at 116 (45) m/sec. This represents an increase of one to two orders of magnitude in total flux above previous cold atomic sources and opens a new regime in the production of ultracold atomic samples.

A picture of the existing experimental set-up is shown in Figure 5, along with a schematic representation of the constituent components. Our source of thermal rubidium atoms originates from a rubidium candlestick atomic beam source (Figure 5a), which provides an intense, well-collimated beam with a mean velocity of 400 m/s. To utilize this source of hot thermal atoms, the beam is first transversely collimated and cooled to remove as much of the initial transverse spread (both in terms of velocity and position) as possible and thus to increase the overall final flux. This is subsequently followed by a Zeeman slower, which serves to longitudinally slow and cool the atomic distribution, as well as to provide us with a means to finely control the final beam velocity.

The initial transverse cooling of the atomic beam employs a novel atomic collimator (Figure 5b), which has a large transverse capture velocity and acts to uniformly decelerate the atoms over its whole length. In the collimator, the 15 cm of transverse collimation is accomplished by two pairs of nearly plane parallel 6 x 1" mirrors (one pair for each transverse axis), with a 1 cm cooling laser coupled in on one side at a small angle relative to the mirror's normal. By using multiple reflections down the length of this cavity, we may effectively apply a cooling force throughout this entire region without the need for excessively large optics or unreasonable power requirements because of the use of light recycling.

By design, as the atomic beam propagates down the collimator, it becomes more and more collimated due to the radiation pressure from the laser beams which become more and more normal to the mirrors by their subsequent reflections. The wavefronts of the collimating laser field are designed to precisely match the deflection/collimation of the atomic beam. In this way, it is possible for the laser beams to remain orthogonal to the trajectory of the atoms, which are then uniformly accelerated radially with the maximum spontaneous force and which, therefore, follow an approximately circular arc. By matching the transverse cooling structure design to the divergence characteristics of the candlestick, we demonstrate that we are able to utilize a full 50% of the atoms emitted from the source for deceleration. As a final consideration, and for fine pointing of the atomic beam, we also employ a 2" region of optical molasses (Figure 5c) at the end of the collimator, increasing the total cooling region's length to a full 8", and meaning we may couple fully 50% of the usable atoms into the next stage of the experiment.

The resulting flux enhancement of the distribution is shown in Figure 6. With the addition of collimation, we are able to increase the flux of atoms arriving in the detection chamber from 2 x 10^{11} atom/s due to the effusion from the candlestick alone to 5.3 x 10^{12} atoms/s. This factor of 25 increase represents fully half of the usable atoms that are emitted from the source. In addition, measurement of the atomic beams transverse velocity spread indicates that the distribution is transversely cooled from 4 m/s RMS (corresponding to that expected for a 400 m/s atomic beam passing through the Zeeman

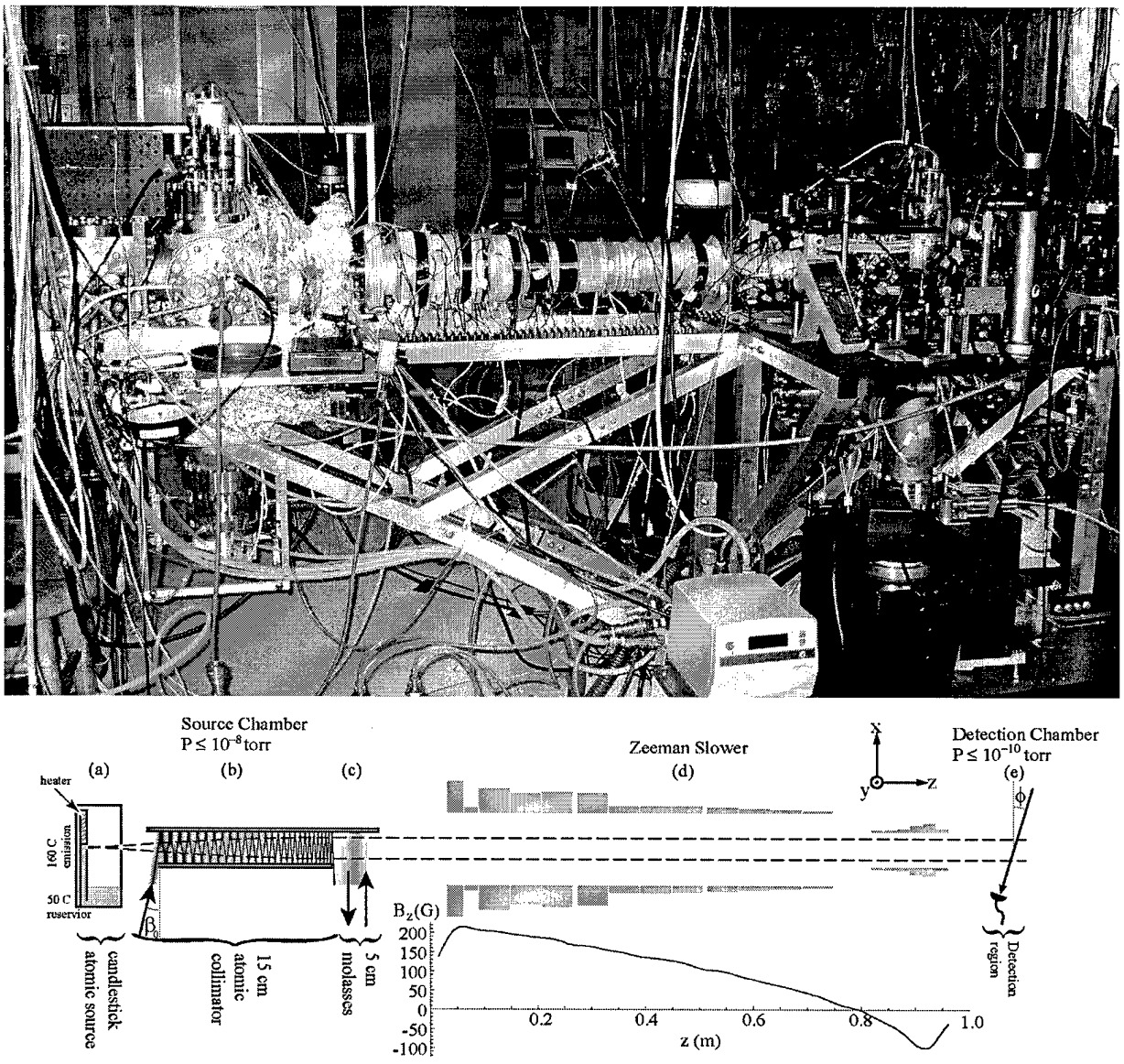

Figure 5 An atomic beam is produced via a candlestick atomic beam source (a) with a divergence angle of 1/10 radian. The atoms in the beam then pass through a 20 cm long transverse collimation (b) and cooling (c) stage and are subsequently longitudinally decelerated and cooled by means of a 1 m long Zeeman slower (d), which is designed in the zero-crossing configuration shown. Measurement of the atomic beam is performed via an absorption measurement 10 cm beyond the end of the Zeeman slower (e).

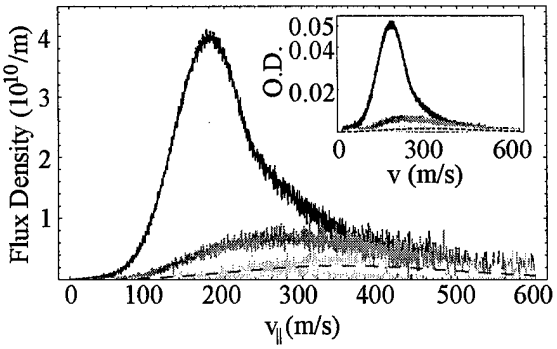

Figure 6. Flux enhancement through transverse collimation and cooling. Flux measured as a function of longitudinal velocity based on measurement of the OD as a function of probe frequency (inset), for the bare atomic beam (light grey) with molasses (dark grey) and with the full 20 cm of transverse collimation and cooling (black). The dashed curve is a calculation of the distribution solely from effusion from the source at T=160° (no adjustable parameters).

slower tube which an aperture defined by a $1/100^{th}$ radian half-angle) to less than 1 m/s. This decrease in spread means that for subsequent beam deceleration, the atomic beam will spread out less, bringing the overall flux enhancement relative to the uncollimated case to a full factor of 50.

Thus, with the atomic beam transversely cooled and collimated, we next cool and decelerate the atomic beam longitudinally by employing a one meter long Zeeman slower, which uses a precisely sculpted magnetic field profile (shown in Figure 5d) to

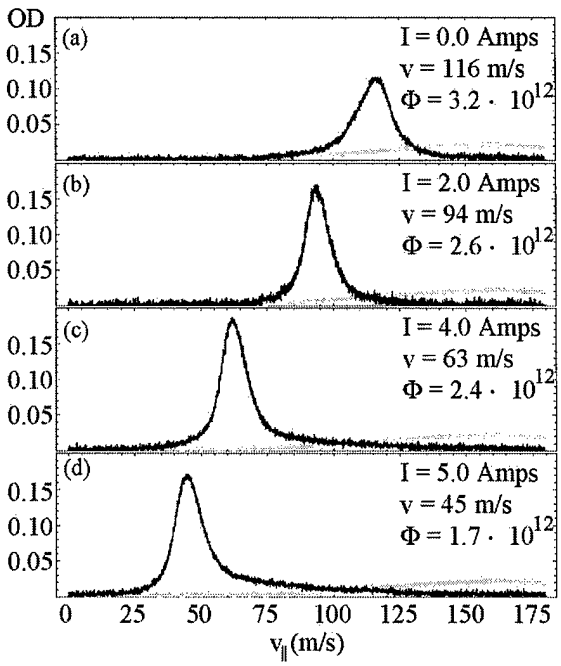

Figure 7: Optical density measurement of Zeeman slowed atomic beam taken at a probe angle of 45° relative to the atomic beam axis for varying final velocities. In all cases, the top thirteen coils of the slower are maintained at I = 5A (corresponding to a capture velocity of 320 m/s). The current in each plot is that of the final set of Zeeman slower coils, which adjust the final velocity by 16 (m/s)/A. The grey curve represents the same situation as the black curve in Fig 2.

compensate for Doppler shifts due to the laser deceleration. The coil design is implemented in two halves, with the top 13 coils (the "positive" part of the slower) setting the maximum capture velocity of the slower, while the final 6 coils (the "negative" part) can be used to set the minimum magnetic field and thus the final velocity of the atoms. Thus, by design, the field allows the velocity of the beam to be controlled to any value between 50-150 m/s, as shown in Figure 7, while still maintaining a flux of 2 x 10^{12} atoms/s or greater.

In addition, with these results in hand, plan to undertake the development of a Monte-Carlo model of the beam source, incorporating the full level structure of rubidium atoms to account for optical and magnetic forces on the atoms. Our success to date with the construction of this source warrants immediate development of several more stages with additional cooling and collimation of the atomic beam, for the ultimate goal of producing a continuously condensed beam of ultracold atoms.

SINGLE ATOM DETECTION OF COLD ATOMS WITH NANOTUBES

Single walled carbon nanotubes have the ability to create enormous electric field (~10V/nm) and magnetic field gradients (~50G/nm) in highly localized regions. The ability to produce large electromagnetic fields with little power dissipation and high localization may well place nanotubes at the heart of a new class of practical devices whose basic operation exploits atomic behavior presently inaccessible to economical portable sensors. Navigational sensors are one class of devices where portability and sensitivity are paramount. Our lab has recently developed the facilities and expertise necessary to produce the nanotube devices that we now have available for experiments with a cold atomic beam.

The initial goal for atom-nanotube study is to develop a high-resolution, low-power, fast, efficient, single-atom detector for cold atoms. A single atom detector would be invaluable in the characterization of cold atomic beams. In addition, a cold-atom source could actually be used to study the fundamental physics of the device itself. We hope to observe the angular momentum

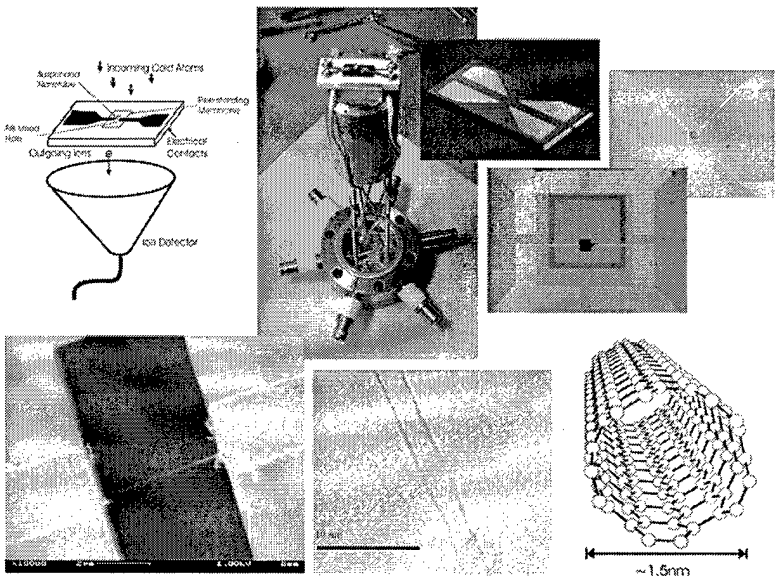

Figure 8: (Top) Schematic of detector, physical implementation, enlarged images of the chip; (Bottom) SEM and TEM images of the nanotube across the gap, rendition of carbon lattice

ladder, a direct consequence of the quantization of angular momentum in quantum systems. Furthermore, the speed and size of the detector make it uniquely suited to measure spatial and temporal coherences in the atomic beam described near the Bose-Einstein phase transition. We suspect the attainment of these goals will eventually lead to the realization of other theoretically predicted effects that include trapping and using cold atoms as a spectroscopic probe for solid state nanostructures.

A schematic of the nanotube single-atom detector is shown in Figure 8 and 9. Cold atoms will be directed towards a single, suspended nanotube, which is supported by a silicon substrate. This nanotube can be floated to several hundred volts (positive) relative to a nearby coaxial grounding cylinder or slightly biased to support generous currents (~25μA) through the nanotube. At reasonably small nanotube voltages (~50V) the electric fields should be sufficient to field ionize nearby rubidium atoms. An electron-multiplier ion detector is directly behind the nanotube in position to detect forward-scattered ions. The detector pulses correspond to individual ions and can be counted with a fast pre-amplifier and counter with time resolution up to about 1ns.

We have developed the preliminary techniques for fabricating this device (Figure 8). The carbon nanotube is grown across an ion-milled gap in a freestanding silicon dioxide membrane supported by a surrounding silicon substrate. [Ref. 7] The suspended nanotube is a few microns long, although we hope to extend this by refining our methods and equipment. Prior to forming the gap, optical lithography is used to pattern a platinum wire approximately 1 μm wide and 100 nm thick across the oxide membrane surface. Several monolayers of iron are evaporated onto the platinum wire to serve as a catalyst for subsequent nanotube growth. A focused ion beam (FIB) is used to cut completely through the metal line and freestanding membrane to yield the gap across which the nanotube is grown. A methane based chemical vapor deposition (CVD) growth method is used to grow nanotubes across the gap from one platinum electrode to the other. The yield of samples with a nanotube bridging the gap and making electrical contact on each side is about 50%. Transmission electron microscope images reveal that the tubes are consistently single walled with 1 nm radii. Growth of longer nanotubes, possibly up to a millimeter, will require a bigger nanotube growth oven with electric feed-thrus for electric-field directionality control.

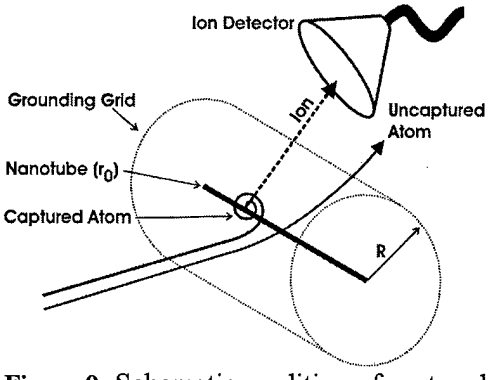

Figure 9: Schematic rendition of captured and uncaptured atoms. Captured atoms undergo field ionization in strong electric fields around the nanotube and are detected.

We anticipate that our studies at these length scales will yield a novel demonstration of fundamental quantum physics in this regime. Far from the tube, the neutral atoms experience a static electric field proportional to nanotube voltage and inversely related to the distance from the nanotube center. The potential energy of a polarizable atom is proportional to the square of the electric field and thus is attractive and has an inverse square radial dependence. Since its first discussion, the attractive inverse square potential has been a fundamental

curiosity of both classical and quantum mechanics. Within the capabilities of our developed device, we have calculated that the detection of quantized angular momentum is realizable [Ref. 8]. The cross-section for atom capture will depend directly on the angular momentum of the incident atom around the nanotube. The critical angular momentum, which sets the threshold between captured and uncaptured angular momentum states, is proportional to the voltage on the nanotube. Therefore, increasing the voltage results in the capture of atoms with increasingly large angular momenta. Classically one expects the capture cross-section to increase linearly with voltage. From a quantum perspective, angular momentum is quantized and the cross-section is expected to increase in discrete steps as each new angular momentum state is captured with increasing voltage. A full quantum mechanical treatment bears out this argument and when the wire diameter is much smaller than the (initial) de Broglie wavelength of the atom, the steps will be sharp and resolvable in a plot of capture cross-section versus voltage. We have determined that the cross-section step heights are proportional to the de Broglie wavelength and the nanotube length, and are spaced approximately every 63 mV, which we have calculated for rubidium atoms and a 2 nm diameter wire. It is important to note that for cold atoms the voltages at which the steps occur are independent of incident atomic velocities.

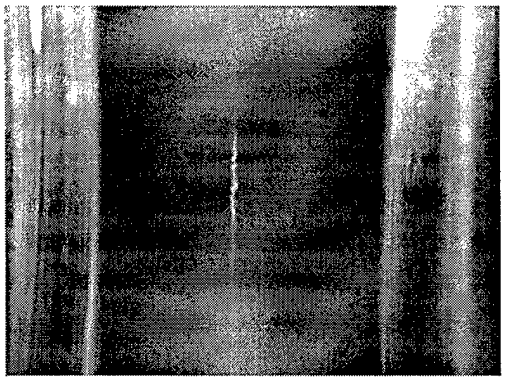

Figure 10: CCD image of the trapped atoms. Laser beam detuning is $-3\,\Gamma$, with zero relative detuning (velocity is zero). Vertical tubing, spaced 1 3/8 inches apart, generates a magnetic field with a gradient of 15 G/cm.

Our completed theoretical investigation yields important insight into the conditions under which steps will be observable. It is paramount that the incident atoms originate from a cold monochromatic atomic source in order for the steps to be visible. Our calculations indicate that velocities below 15 m/s are appropriate for these measurements.

To obtain a cold atomic beam with this characteristic velocity, we are in the process of constructing and optimizing a magneto-optical trap. A magnetic field confines the atoms in the horizontal plane but not in the vertical direction, which creates a narrow beam of atoms that can be launched vertically by detuning the relative frequencies of the laser beams. Our preliminary measurements of this MOT have been performed primarily with a CCD camera (Figure 10) and we are currently pursuing quantitative measurements of the basic atomic beam parameters.

This detection mechanism offers particular exciting possibilities when used as a wavefunction microscope to image a BEC. One can imagine using the nanotube to ionize atoms out of the condensate in pulsed mode where the cloud is dropped onto the tube. The spatial pattern of ions (accessible with a multi-channel plate) reflects the condensate wavefunction at length scales well below optical wavelengths, a regime never-before seen.

[Ref. 1] N. S. Ginsberg, J. Brand, and L. V. Hau, submitted to Phys. Rev. Lett., e-print: cond-mat/0408464 (2004).

[Ref. 2] L. V. Hau, S. E. Harris, Z. Dutton and C. H. Behroozi, Nature **397**, 594 (1999).

[Ref. 3] Z. Dutton, M. Budde, C. Slowe, and L. V. Hau, Science **293**, 663 (2001), and Science Express, June 28 2001 (<zdoi;10.1126/science.1062527>).

[Ref. 4] C. Liu, Z. Dutton, C. H. Behroozi and L. V. Hau, Nature **409**, 490 (2001).

[Ref. 5] Z. Dutton, N. S. Ginsberg, C. S. Slowe and L. V. Hau, Europhysics News, March/April Issue, 33 (2004). Cover.

[Ref. 6] C. Slowe, L. Vernac, and L. V. Hau, Available on xxx.lanl.gov article arXiv:physics/0407040v1 4 Jul 2004. To be sumbmitted to *Review of Scientific Instruments.*

[Ref. 7] H. B. Peng, T. G. Ristroph, G. M. Schurmann, G. M. King, Joonah Yoon, V. Narayanamurti, J. A. Golovchenko. *Applied Physics Letters* **83**, 4238 (2003).

[Ref. 8] T. G. Ristroph, A. L. Goodsell, J. A. Golovchenko, L. V. Hau, *accepted for Physical Review Letters.*